A Signal Transduction Pathway Model Prototype I: From Agonist to Cellular Endpoint

Thomas J. Lukas
Department of Molecular Pharmacology and Drug Discovery Program, Northwestern University, Chicago, Illinois

ABSTRACT The postgenomic era is providing a wealth of information about the genes involved in many cellular processes. However, the ability to apply this information to understanding cellular signal transduction is limited by the lack of tools that quantitatively describe cellular signaling processes. The objective of the current studies is to provide a framework for modeling cellular signaling processes beginning at a plasma membrane receptor and ending with a measurable endpoint in the signaling process. Agonist-induced Ca^{2+} mobilization coupled to down stream phosphorylation events was modeled using knowledge of in vitro and in vivo process parameters. The simulation process includes several modules that describe cellular processes involving receptor activation phosphoinositide metabolism, Ca^{2+}-release, and activation of a calmodulin-dependent protein kinase. A Virtual Cell-based simulation was formulated using available literature data and compared to new and existing experimental results. The model provides a new approach to facilitate hypothesis-driven investigation and experimental design based upon simulation results. These investigations may be directed at the timing of multiple phosphorylation/dephosphorylation events affecting key enzymatic activities in the signaling pathway.

INTRODUCTION

Regulation of cell function involves the simultaneous operation of multiple signaling pathways that translate signals (extracellular and intracellular) into cellular responses. In the postgenomic era, components of signal transduction pathways are being elucidated by genomic and proteomics methods. Although this information allows the creation of testable pathway maps, the details of the signal transduction pathway (kinetics, feedback, and concentration dependencies) are poorly understood because there are many variables and conditions that need to be integrated (Slepchenko et al., 2002; Bray, 1997). How the cellular biochemistry is coordinated to define a process operation remains a large problem. Another complication is that different cell types may have common signal transduction pathways, but the details leading to the endpoints of these paths may be different. Therefore, we should expect that parameters controlling a cellular signaling process are fine-tuned to specific functional requirements. Without quantitative models, the methods to obtain these parameters are limited. Traditionally, a logical guess is made as to the importance of a component and by pharmacological intervention or genetic manipulation, the component is perturbed and the resulting effects on the system observed. The problem is that this one-at-a-time approach is time-consuming and usually not quantitative. Biological systems analysis through computer simulation offers one way to integrate proposed models or signal transduction maps, and empirical data to formulate complex systems so that ''what if'' questions may be asked ahead of experimental execution. Mathematical formulations and computer programs that simulate signaling fluxes, enzyme kinetics, and metabolism have been described and validated. Thus, the task at hand is to take advantage of these tools to construct quantitative simulation models that will allow the testing of hypotheses that arise from observations of cellular pathology or effects of various external stimuli on gene expression and cellular function.

In the current effort, the Virtual Cell simulation and analysis suite was used to develop a complete agonist-initiated signaling and biological response system. Using existing Virtual Cell models that include phospholipid (Xu et al., 2003) and Ca^{2+} mobilization modules (Fink et al., 1999, 2000), new modules for modeling the upstream events that trigger agonist-induced Ca^{2+} mobilization were coupled to downstream events of Ca^{2+} signaling and measurable endpoints. A generic Ca^{2+} signaling model based upon existing G-protein-coupled receptor (GPCR) models for the purine receptor (Lemon et al., 2003a,b) and chemokine receptors (Riccobene et al., 1999; Adams et al., 1998; Shea and Linderman, 1997) was developed. Models were refined using existing experimental dose/response data obtained with various ligands. (Monck et al., 1988; Moneer and Taylor, 2002; Marsh and Hill, 1993; Leeb-Lundberg et al., 2001; Schaeffer et al., 2001). Thus, this new model is applicable to a variety of Ca^{2+}-mobilizing agonists by using receptor-specific parameters that are obtainable from existing literature or from readily designed experiments. The ligand-receptor activation model and parameters for processes that generate second messengers (inositol tris 1,4,5 -phosphate (IP3) and Ca^{2+}) were then coupled to a prototypical downstream process: Ca^{2+}-mediated initiation of smooth muscle contraction via the phosphorylation of myosin II. Extensive experimental work has been done on the myosin-mediated

Submitted September 29, 2003, and accepted for publication May 4, 2004.

Address reprint requests to Prof. Thomas J. Lukas, Dept. of Molecular Pharmacology and Biological Chemistry, Northwestern University, Ward 8-200, 303 E. Chicago Ave., Mail Code S-215, Chicago, IL 60611. Tel.: 312-503-0847; E-mail: t-lukas@northwestern.edu.

0006-3495/04/09/1406/11 $2.00

doi: 10.1529/biophysj.103.035253

process in various cell types and many of the components and parameters needed for modeling have been reported. However, what is needed is the formulation of an in silico simulation that includes a continuous path of coupled components. Although the network of interconnected signaling pathways is complex, the current results demonstrate that appropriately selected parameters allow successful modeling of a prototypical Ca^{2+} signal transduction process. Additionally, scientific insights can be realized by executing the simulation process leading to new hypotheses that can be tested experimentally.

METHODS

Model strategy and construction

A schematic of the agonist-induced Ca^{2+} signaling process is illustrated in Fig. 1. The prototype is a smooth muscle cell that includes GPCRs for agonists such as bradykinin, angiotensin II, etc. The primary events leading to Ca^{2+} mobilization by such agonists are mediated by the activation of phospholipase C (PLC) that hydrolyzes the lipid, phosphatidylinositol 4,5 phosphate (PIP2) to generate IP3. IP3 then diffuses through the cell to the endoplasmic reticulum (ER) and binds to the IP3-receptor channel that releases Ca^{2+} from the ER. In the current model the downstream event involves the Ca^{2+} effector calmodulin (CaM), its binding to myosin light chain kinase (MLCK), activation of the CaM:MLCK complex, and phosphorylation of the regulatory myosin light chain (MLC) that initiates contraction in smooth muscle and motility in nonmuscle cells. Also included are several control elements that are involved in regulating the level and duration of MLC phosphorylation. These control elements include regulation of MLCK by other protein kinases, the dephosphorylation of myosin light chains by MLC phosphatase (MLCP), and both up- and down-regulation of this phosphatase activity. These elements are necessarily complex and not completely understood, because several protein kinases and signaling networks are involved in regulating MLC phosphatase activity. However, the advantage of using a simulation environment is that control elements can be modified as needed. It is envisioned that other Ca^{2+}-mediated downstream processes such as secretion and gene transcription can be modeled in a similar fashion. Agonist and cell-type specific parameters may be added by using the generated templates within the Virtual Cell system (www.nrcam.uchc.edu). Alternatively, the system (including the generated ordinary differential equations) can be exported to other simulation programs by way of the export functions on the XML part of the Virtual Cell model page. Thus, the simulation suite is designed to be portable and available to a wide variety of researchers. All simulations presented in this work used the Runge-Kutta fourth-order solver with a fixed time step of 0.1 ms. The Virtual Cell biomodel can be found in the public directory Ca_release_coupled_MLC.

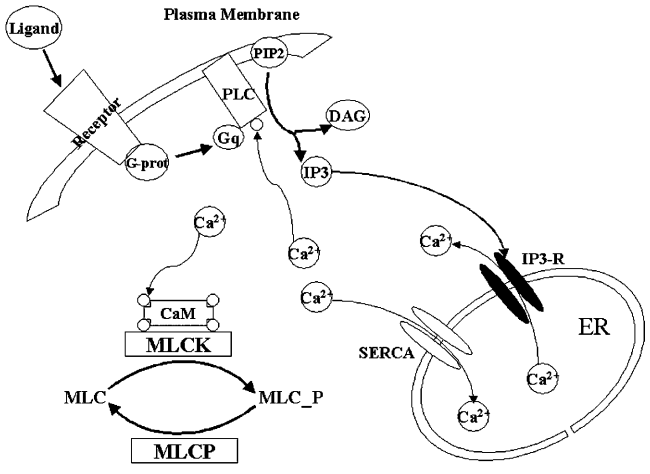

FIGURE 1 Three-compartment cell model containing plasma membrane, cytoplasmic reticulum, and ER. The primary activities modeled using the Virtual Cell are the GPCR-mediated activation of phospholipase C, Ca^{2+} release and uptake in the ER, and activation of the CaM-MLCK complex.

Prototype model for agonist-coupled Ca^{2+} signaling

The model design (Fig. 1) contains three compartments, plasma membrane, cytosol, and ER. The volume ratio ER/cytosol is 0.15, typical of cultured cells with a total cell volume of 1×10^{-15} cm^3 employed in most cell model systems (Slepchenko et al., 2002; Fink et al., 1999; Lemon et al., 2003b; Riccobene et al., 1999). The plasma membrane is the starting point for the design of the system. It contains a G-protein-coupled receptor, PLC and other lipid transforming enzymes. To simplify the overall system the plasma membrane Ca^{2+} channels and efflux pumps were not implemented so that only IP3-generated Ca^{2+} fluxes arising from the ER compartment are used. For systems where Ca^{2+} and other ion channel(s) activated by agonists are important, these features may be added as needed. However, the simplification offered in the current model is justified because other model systems dealing with IP3-generating and Ca^{2+}-release modules have been successful at explaining experimental data with this closed system (Lemon et al., 2003a; Fink et al., 2000; Shea and Linderman, 1997).

Plasma membrane components: G-protein-coupled receptor formulation

The formulation of agonist-mediated signaling through G-protein-coupled receptors is based upon modern receptor theory (Kenakin and Onaran, 2002; Kenakin, 1997, 2002) guided by existing treatments for receptors coupled to heterotrimeric G-proteins containing the Gq subunit that activates phospholipase C and downstream signaling. A generic GPCR receptor model (Riccobene et al., 1999; Kenakin, 2002) is shown in Fig. 2. This model includes the concept of receptor coupling G-protein and ligand in a complementary fashion that enhances the response of the ligand (L) (Eq. 1) (Kenakin, 2002):

$$\text{Response} = e[L]/([L] + K\text{d}). \tag{1}$$

The enhancement obtained depends upon the concentration of G-protein and its affinity for the receptor in the presence and absence of ligand (Fig. 2). In the model, two receptor species (R^* and R) representing G-protein-coupled and uncoupled species interact with ligand (L). Receptors bound to the G-GDP heterotrimeric complex (R^*) are assumed to be in their high-affinity state (coupled receptors), whereas uncoupled (R) are lower affinity. The coupling factor, α, is applied to the forward rate constant (kf) for ligand binding to ''coupled receptor.'' Ligand also binds to uncoupled receptor that then engages G-protein complex with α applied to Kact, the receptor activation constant. The ternary complex (receptor bound to both ligand and G-protein) as a ratio (ρ) of total receptor is given by Eq. 2 (Kenakin and Onaran, 2002):

$$\rho = \frac{K\text{act}(1 + \alpha[L]/K\text{d})}{[L]/K\text{d}(1 + \alpha K\text{act}) + K\text{act} + 1.} \tag{2}$$

$$\rho = \alpha(1 + K\text{act})/(1 + \alpha K\text{act}) \tag{2.1}$$

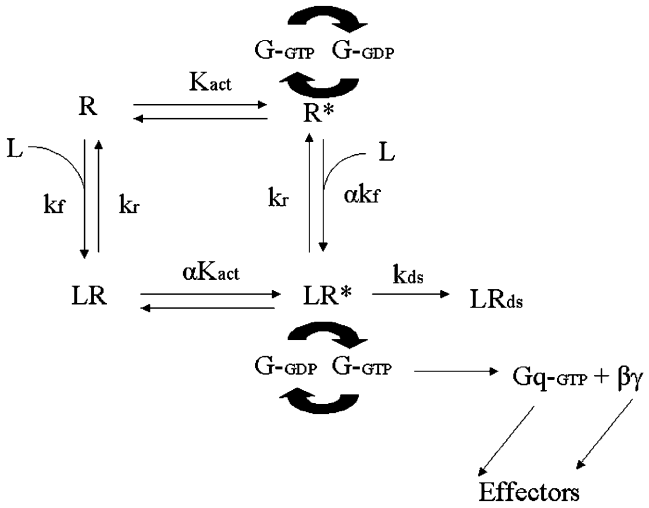

FIGURE 2 Generic GPCR receptor model details. The model is based upon the precoupled receptor concept (Shea and Linderman, 1997) including high-affinity coupled (R^*) and low-affinity uncoupled (R) receptors for ligand (L) binding.

In the absence of ligand, Eq. 2 reduces to Eq. 2.1, where ρ represents the fraction of precoupled receptors. Previous modeling of complexes for typical GPCRs indicated that a range of 10–30% of the receptors may be precoupled to G-protein (Shea and Linderman, 1997). In the current generic model, the fraction of precoupled receptors was set within this range by the values of α and Kact. In the ternary complex (LR^*), G-protein exchanges GDP for GTP, followed by G-protein complex dissociation. In the current simplified model, constitutively active receptors are ignored as they are assumed to have low intrinsic GTP exchange activity in line with experimental data (Shea and Linderman, 1997). However, constitutively active GPCR mutants are known (Parnot et al., 2002), so that these species can be activated if needed. Desensitization of the activated receptor was modeled as an irreversible phosphorylation (rate constant = kds) by a G-protein receptor kinase (GRK) that inactivates further signaling (Kenakin, 1997; Woolf and Linderman, 2003). The decay of the activated Gq through GTP hydrolysis eventually terminates the generated signal. Table 1 summarizes ligand binding and dose-response information about specific Gq coupled receptors. A highly coupled system ($\alpha > 10$) will generate the maximal amount of activated Gq. Inspection of the data on some GPCR receptors (Table 1) indicates that the EC50 of Ca^{2+} or downstream events is usually less than the Kd of the ligand for the receptor, suggesting coupling of the signaling process. However, data for some agonists, such as bradykinin B2 and Arg-vasopressin receptors is different because the EC50s are greater than the Kd of the ligand. This does not necessarily mean that there is no coupling, but suggests that a process downstream of the ligand-receptor-G-protein complex is low efficiency. For example, this could be due to the inactivation of G-protein signaling by the activity of RGS proteins that bind activated G-proteins and catalyze GTP hydrolysis (Zhong et al., 2003; Woolf and Linderman, 2003). The generic model contains 20,000 receptors and 100,000 heterotrimeric G-proteins per cell. The ligand-binding constant (Kd) is 0.01 μM, and the coupling factor $\alpha = 1000$. Appendix A contains the formulations (Eqs. A1–A3) used in the Virtual cell that describe receptor activation and generation of activated G-protein, Gq-GTP.

Phosphatidyl-inositol synthesis

Fig. 3 illustrates the details of the phosphoinositide synthesis and generation of the messengers diacylglycerol (DAG) and IP3 by phospholipase C. It has been established that agonist-mediated Ca^{2+} signaling involves more than just the activation of phospholipase C, because pools of its substrates within the plasma membrane are finite (Toker, 1998). Thus, for sustained agonist stimulation and signaling, continuous synthesis of the PLC substrate (phosphatidyl-4,5, bisphosphate, PIP2) and upstream precursors must occur (Toker, 1998; Weernink et al., 2000; Rumenapp et al., 1998). Although the enzymes that participate in PIP2 synthesis are known (Fig. 3), their regulatory paradigm with regard to GPCRs is not clear. Experimental evidence implicates Rho GTPases (Weernink et al., 2000; Rumenapp et al., 1998; Schmidt et al., 1996) and activation by selected lipid products (Moritz et al., 1992) as participants in modulating PIP2 levels. Previous modeling efforts in this regard employed a resynthesis factor coupled to IP3 production to replenish PIP2 consumed by PLC (Lemon et al., 2003b), stimulated and basal synthesis factors (Xu et al., 2003), and a feedback network based upon synthesis of other inositol phosphates downstream of IP3 (Mishra and Bhalla, 2002). Among these options, an existing Virtual Cell model (Xu et al., 2003) provided a reasonable approach to this problem. First, a basal synthesis term (Vbasal) is activated if PIP2 falls below a preset level. This strategy allows replenishment of PIP2 after agonist stimulation, typically within a few minutes. The second term is a stimulation of PIP2 synthesis (Vstim) during the peak of PIP2 consumption by PLC. This allows a bolus of PIP2 to become available during the peak of IP3 synthesis and prevents complete depletion of the PIP2 supply. These terms were combined as and expressed as exponentials as shown in Eqs. A4 and A5–A6 (Appendix).

Phospholipase C activation

PLC is expressed as several isoforms that exhibit differential sensitivity to Gq and $\beta\gamma$ G-protein subunits as well as Rho GTPases (Rhee and Bae, 1997). The PLCβ1 and PLCβB2 isoforms are the primary transducers of Gq-mediated signals in the central nervous system and smooth muscle cells, whereas PLCβ3 transduces $\beta\gamma$ signals and is found in myeloid cells (Illenberger et al., 2003). Formulation of PLC activity was based upon the kinetic parameters found with reconstituted PLCβ1 (Mukhopadhyay and Ross, 1999; Smrcka et al., 1991). Two convergent paths were used to generate full PLC activity (Fig. 4). These involved the sequential activation

TABLE 1 Ligand binding and dose/response data for some Ca^{2+} mobilizing GPCRs

Receptor	Ligand Kd (nM)	EC50 (nM) Ca^{2+} response or activity (–)	References
Generic	10	3	See Text
Bradykinin B1	7000	300	(Leeb-Lundberg et al., 2001)
Bradykinin B2	0.3	2	(Marsh and Hill, 1993; Schaeffer et al., 2001)
Chemokine pep1	4.4	0.4–	(Riccobene et al., 1999; Adams et al., 1998)
Chemokine pep2	60	60–	(Riccobene et al., 1999; Adams et al., 1998)
Purine-P2Y2(UTP)	5000	250	(Garrad et al., 1998)
Endothelin		0.5–70	(Muldoon et al., 1989; Takuwa et al., 1990)
Arg Vasopressin	0.5	1–19	(Monck et al., 1988; Moneer and Taylor, 2002)

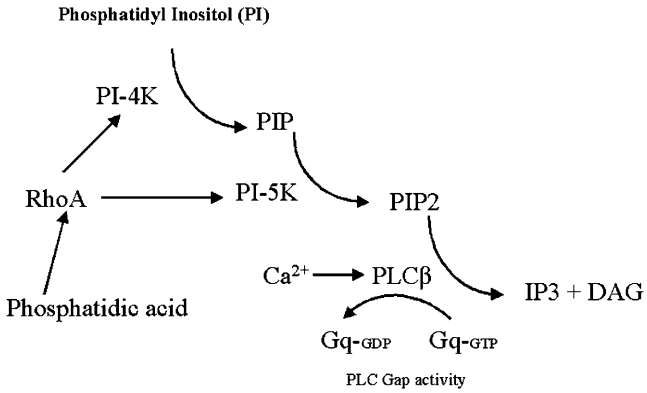

FIGURE 3 Phospholipid synthesis cascade. In the model, the phosphatidylinositol (PI) and phosphatidyl 4-phosphate (PIP) are fixed. The PLC substrate, phosphatidylinositol 4,5-bisphosphate (PIP2) is synthesized at a combined basal and stimulated rate from PIP. (See Eqs. 6–7).

of PLC by Gq-GTP and Ca^{2+} to generate the active enzyme Ca^{2+}-PLC–Gq-GTP. Under resting conditions, PLC is distributed between native and Ca^{2+}-bound forms as established by the equilibrium constant *K*c-plc-b (~1 μM)(Smrcka et al., 1991). As Gq-GTP is generated, both forms proceed to form the active complex. However, because of thermodynamic coupling, Ca^{2+} binds to PLCβ-Gq with higher affinity than PLCβ alone (*K*c-plc-s = 0.1 μM) (Smrcka et al., 1991). Similarly, the rate constant for the Gq-GTP activation of Ca^{2+}-PLCβ is 10-fold higher than the apoenzyme (Table 2). PLC enzymatic activity is down-regulated through GTP hydrolysis within the complex. The rate of this GTPase activity (6/s) is significantly faster than the basal GTPase activity of Gq (0.15/s) due to the GAP (G-protein activating protein) activity of PLC (Mukhopadhyay and Ross, 1999). Thus, it is assumed that the activated complex Ca^{2+}-PLCβ-Gq-GTP is responsible for most of the stimulated PLC activity. Because Ca^{2+}-PLCβ has a somewhat lower specific activity than the Gq-activated form (Smrcka et al., 1991), this species is a minor contributor to PLC activity and in the current model formulation provides the basal activity. Eqs. A7 and A8 (see Appendix) describe the PIP2 hydrolysis steps carried out by PLCβ

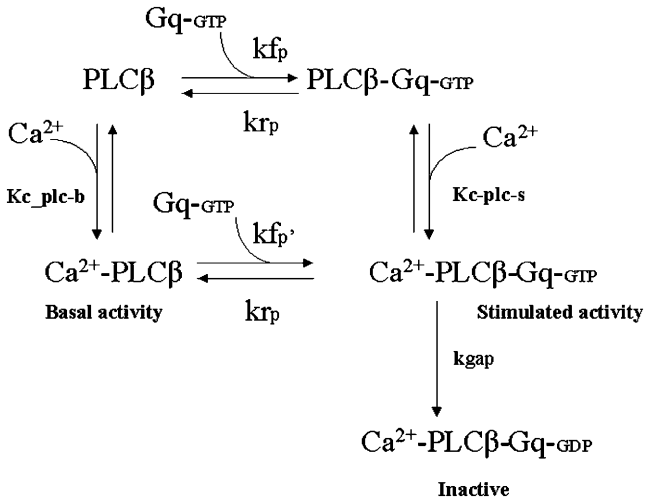

FIGURE 4 Activation of PLC by dual pathways. The Ga subunit Gq-GTP interacts with PLC to form active complex PLCβ-Gq-GTP that has high affinity for Ca^{2+} thus creating the active enzyme Ca^{2+}-PLCβ-Gq-GTP that hydrolyzes PIP2 to DAG and IP3 (Fig. 3). Ca^{2+}-PLCβ provides the basal activity in the absence of activated Gq proteins.

providing stimulated and basal levels of IP3. The kinetic parameters used for these processes are summarized in Table 2.

ER compartment

The intracellular Ca^{2+} compartment (ER) contains the IP3 release channel, and the ER Ca^{2+} pump (SERCA). There are several mathematical models (Schuster et al., 2002; Goldbeter et al., 1990; Li and Rinzel, 1994) for dealing with IP3-generated intracellular Ca^{2+} fluxes. Some of these models allow for oscillations in Ca^{2+}, whereas others do not. The model used for a smooth muscle prototype is nonoscillatory under normal IP3 and Ca^{2+} flux conditions (Fink et al., 1999). The IP3-mediated Ca^{2+} release and SERCA activities are derived from minimal variable formulations (Li and Rinzel, 1994; Keizer and De Young, 1994) as implemented by Loew and co-workers in the Virtual Cell (Fink et al., 1999, 2000).

Cytoplasmic compartment

Ca^2, CaM-complexes, and the activation of MLCK

The participating elements in the MLCK module are illustrated in Fig. 5. The active Ca^{2+}-CaM-MLCK complex is generated from two paths similar to PLCβ (Fig. 3). In the first, preformed complexes of CaM and MLCK bind Ca^{2+} and are activated. In the second path, the Ca^{2+}-CaM complex binds to MLCK forming the same active complex. Estimates of the affinity of CaM and MLCK in the absence of, or low, Ca^{2+} conditions vary widely. Peptide analogs of the CaM binding domain of MLCK interact with CaM in the absence of Ca^{2+} with an ionic strength-dependent *K*d of 5–270 μM. CaM-MLCK complexes have also been detected at very low Ca^{2+} (Wilson et al., 2002; Milos et al., 1988). Thus, preformed CaM-MLCK complexes were included in the formulation of MLCK activation. The CaM-MLCK equilibrium constant was set at 27 μM, as a lower limit assuming that the ionic strength within the cytoskeletal environment is favorable for complex formation. Using this value, 0.36 μM CaM-MLCK complex is formed at equilibrium with 1 μM CaM and 10 μM MLCK (Taylor and Stull, 1988). This amount of CaM-MLCK complex represents ~11% of the CaM retained in cytoskeletal cell fractions (Wilson et al., 2002). Ca^{2+} binding to CaM in the presence and absence of target proteins was formulated as mass action equilibria (Eq. 3), with an exponent, *n*, on the Ca^{2+} corresponding to the Hill coefficient for binding derived from modified Adair-Klotz equations that account for coupling between target binding and Ca^{2+} to CaM (Haiech et al., 1991; Mirzoeva et al., 1999):

$$Ca^{2+}\ \text{binding rate} = k\text{f}Ca[CaM][Ca^{2+}]^n - k\text{r}Ca[Ca^{2+}\text{-CaM}]. \quad (3)$$

CaM-MLCK complexes were formulated similarly, except that CaM in Eq. 3 is replaced by CaM-MLCK. The on/off rates for Ca^{2+} to CaM in the presence and absence of MLCK were adjusted based upon in vitro measurements found in the literature (Johnson et al., 1996; Black et al., 2000). Similarly, on/off rates for Ca^{2+}-CaM binding to MLCK were based upon available in vitro data (Johnson et al., 1996; Kasturi et al., 1993). Because the off-rate of Ca^{2+} from CaM and CaM-target complexes is biphasic (Kasturi et al., 1993), an average value was used. Relevant parameters used in the simulation are in Table 3. Simulations were begun with equilibrium values for CaM-MLCK, CaM-buffer protein, and Ca^{2+}-CaM-MLCK complex obtained by running simulations for several minutes without IP3 generation. Myosin light chain concentration was set at 24 μM. A modified Michaelis-Menton equation (Eq. 4) with explicit enzyme concentration (Mendes, 1997) was used for MLCK activity based upon the level of Ca^{2+}-CaM-MLCK complex:

$$\text{Rate} = K\text{cat}[\text{enzyme}][\text{substrate}]/(K\text{m} + [\text{substrate}]). \quad (4)$$

TABLE 2 Phospholipase C IP3/DAG parameters

Reaction	*K*d μM	*k*f 10^6 M^{-1} s^{-1}	*k*r s^{-1}
PLC + Gq-GTP → PLC-Gq-GTP		0.0042	1
PLC + Ca ↔ Ca^{2+}-PLC	1.0		
PLC-Gq-GTP + Ca^{2+} ↔ Ca^{2+}-PLC-Gq-GTP	0.1		
Ca^{2+}-PLC + Gq-GTP → Ca^{2+}-PLC-Gq-GTP		0.042	1
PIP2 + Ca^{2+}-PLC-Gq* → DAG + IP3	*K*cat = 50/s		
PIP2 + Ca^{2+}-PLC → DAG + IP3 (basal)		0.0002	1
Ca^{2+}-PLC-Gq* → Ca^{2+}PLC + Gq		6 /s	
IP3-deg		1.25/s	
DAG-deg		0.15/s	

Parameters are based on work by Sivakumaran et al. (2003) and Smrcka et al. (1991).

MLCP and regulatory elements

The myosin light chain phosphatase kinetic parameters were based upon in vitro measurements of the phosphorylated and nonphosphorylated enzyme where the phosphorylated form has a fraction (0.07–.2) of the specific activity of the unphosphorylated species (Table 3). More details on the regulation of MLCP by phosphorylation and inhibitory proteins is in the companion article (Lukas, 2004). These include phosphorylation of the regulatory subunit (MYPT), activation of the phosphatase inhibitor (CPI-17), and cyclicGMP-mediated inhibition of MYPT phosphorylation.

RESULTS

Generic model

In a typical simulation using the generic model, binding of ligand to GPCR increases the level of active Ca^{2+}-CaM-MLCK complex after the rise in IP3 and Ca^{2+}(Fig. 6 *A*). A ligand (*K*d = 10 nM) at a concentration of 100 nM causes a Ca^{2+} flux that peaks at 0.71 μM, comparable to the range of 0.25–0.85 μM measured in smooth muscle cells (Simpson and Ashley, 1989; Taylor and Stull, 1988; Willars et al., 1998). The ultimate Ca^{2+} peak also depends upon the level of Ca^{2+} buffering. In this smooth muscle cell model, a single buffer was used at a concentration of 350 μM and a *K*d of 10 μM (Fink et al., 1999). Reducing the Ca^{2+} buffer concentration fourfold to 87.5 μM increases the peak Ca^{2+} to 1 μM. Thus, the peak Ca^{2+} is relatively insensitive to Ca^{2+} buffer concentration within the range tested. Activated CaM-MLCK complex peaks at ~2 μM, or ~20% of the total MLCK. The Ca^{2+} output is also limited by the IP3 production that maximizes at 1.1 μM. The IP3 receptor Ca^{2+} release parameters for smooth muscle cells (Fink et al., 1999) make the channel more sensitive to IP3 than in neuronal cell models (Fink et al., 2000). The ligand dependence of peak Ca^{2+} in the model simulations is shown in Fig. 6 *B*. The profile parallels that observed for bradykinin stimulated smooth muscle cells (Fig. 6 *B*, *inset*). In an expanded view of the IP3 and Ca^{2+} release (Fig. 7), the profiles are biphasic. This result was expected because the initial fast phase of Ca^{2+} release follows the peak of IP3 synthesis when the PIP2 supply is maximal, whereas the second phase (not a plateau) reflects sustained release at a lower IP3 synthesis rate as PIP2 resynthesis occurs (Fig. 7 *B*). Compared to data from Arg-vasopressin treated vascular smooth muscle cells in the absence of extracellular Ca^{2+} (Simpson and Ashley, 1989) (Fig. 7 *A*), the simulation data exhibit a faster rise in Ca^{2+}, but the second phase and decay are similar. In a study of smooth muscle cells treated with the Ca^{2+} mobilizing agonist, carbachol (Willars et al., 1998), the stimulated IP3 production and Ca^{2+} levels exhibited a rapid peak followed by a second slower phase that was eliminated when cells were pretreated with wortmannin, an agent that inhibits PI-4 kinase in the PIP2 synthetic pathway (Fig. 3). Therefore, the Gq-GTP-activated PLC, IP3 generation, PIP2 replenishment, and Ca^{2+} release parameters used in the simulation adequately describe these processes in living cells. The use of precoupled receptors (see above) may be partly responsible for the faster rise in IP3 and Ca^{2+} in the simulation results because without precoupling, the Ca^{2+} peak shifts to the right (Fig. 7 *A*). Thus, the delay in Ca^{2+} generation observed experimentally may be due to differences in receptor precoupling and/or receptor number

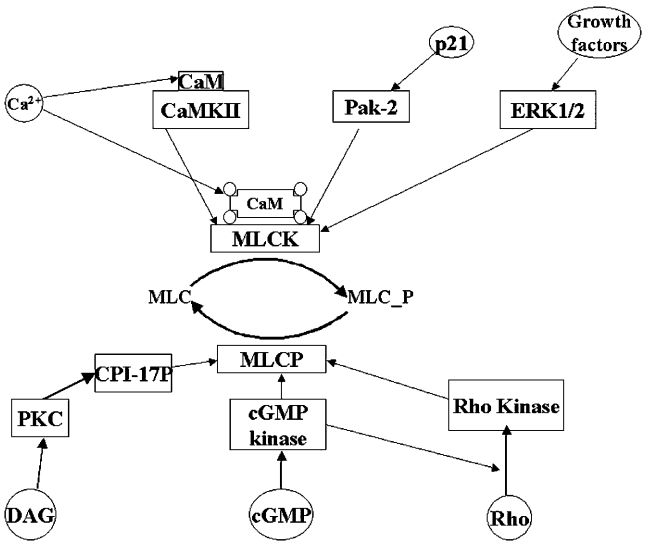

FIGURE 5 Ca^{2+}-calmodulin-associated signaling elements. Shown are the details of the MLC phosphorylation/dephosphorylation module. The model and simulation system contain dynamic regulation of MLCK and MLCP activities through second messenger-mediated phosphorylation/dephosphorylation events. The effectors are shown in boxes and second messengers in circles.

TABLE 3 Ca^{2+}, CaM, MLCK, PKC, and MLCP parameters

Reaction	*K*d (μM)	*k*f (on-rate) M^{-1} s^{-1}	References
MLCK + CaM ↔ CaM-MLCK	27	5	(Tsvetkov et al., 1999), see text
$4Ca^{2+}$ + CaM-MLCK ↔ Ca^{2+}-CaM-MLCK	0.5*	7.5*	(Tansey et al., 1994; Johnson et al., 1996; Sivakumaran et al., 2003)
CaM + $4Ca^{2+}$ ↔ Ca^{2+}-CaM	2.5	12*	(Davis et al., 1999; Johnson et al., 1996; Black et al., 2000)
Ca^{2+}-CaM + MLCK ↔ Ca^{2+}-CaM-MLCK	0.0011	28	(Johnson et al., 1996; Kasturi et al., 1993)
Ca^{2+}-CaM + MLCK-P ↔ Ca^{2+}-CaM-MLCK-P	0.023	8	(Johnson et al., 1996; Kasturi et al., 1993)
Enzyme kinetics	*K*m μM	*K*cat s^{-1}	
Ca^{2+}-CaM-MLCK + MLC → MLC-P	10	27	(Ikebe and Reardon, 1990)
MLCP + MLC-P → MLC	15	16	(Feng et al., 1999; Ichikawa et al., 1996)
MLCP-P + MLC-P → MLC	58	2.1	(Feng et al., 1999; Ichikawa et al., 1996)

*Values were optimized by comparison to experimental data.

per cell (compared to the generic model). Thus, to achieve a closer correspondence between simulation predictions and experimental data, the simulation parameters must be optimized for a specific agonist and cellular background (see below).

To investigate the dynamic range of the generic model, the time course of MLC phosphorylation was simulated for ligand concentrations of 3–300 nM, assuming a *K*d of 10 nM). Fig. 8 illustrates the results obtained from such a simulation. As the ligand concentration increases, both the peak concentration of phosphorylated MLC and the time frame are affected. The lowest ligand concentration exhibits a peak at 15 s, whereas the higher ligand concentrations peak at 4–8 s. These differences are a result of the timing of multiple phosphorylation events (on the regulatory subunit of MLCP or the inhibitory protein CPI-17) that either precede or are coincident with MLC phosphorylation. How these events affect the overall response of the system is further investigated in the accompanying article (Lukas, 2004).

Modeling of bradykinin receptors

Using the generic GPCR model as a template, the model was applied to Ca^{2+}-mobilizing bradykinin receptors to test the simulation system. The bradykinin B2 receptor is a high-affinity species that is widely distributed, whereas the B1 receptor is lower in affinity and abundance in most smooth muscle tissues, but may be up-regulated during inflammatory conditions (Leeb-Lundberg et al., 2001). How the Kd of the receptor changes the response of the simulation system is shown in Fig. 9. In these simulations, the bradykinin B2 receptor (Kd = 0.3 nM) is compared to the bradykinin B1 receptor (Kd = 7 μM) over a ligand concentration range of 0.01–10 μM. The predicted EC50 (peak Ca^{2+} response) for the B2 receptor is 2.2 nM (Fig. 9 *A*), whereas the B1 receptor is 0.78 μM (Fig. 9 *B*) (compare to Table 1: 2 nM and 0.3 μM, respectively). Thus, the low-affinity B1 receptor is not accurately modeled with the current system parameters such as the receptor G-protein coupling or the ligand binding on-rate. Because the binding kinetics for B1 receptors varies with ligand (Leeb-Lundberg et al., 2001; Schaeffer et al., 2001), the EC50 for Ca^{2+} mobilization may be due to a difference in receptor binding kinetics. A fivefold enhancement of ligand on-rate was applied to both the precoupled receptor R^* and the uncoupled receptor R (Fig. 2). Now the predicted Ca^{2+} and active CaM-MLCK complex formation from ligand binding at the B1 receptor has ligand dependence as shown in Fig. 9 *C* and exhibits an EC50 of 0.24 μM (peak Ca^{2+} response), more consistent with experiment. Another important difference between the bradykinin receptors is that the B1 receptor is not down-regulated through a phosphorylation mechanism (Leeb-Lundberg et al., 2001) so that its desensitization is slower than the B2 receptor. To determine the characteristics of a cell containing both receptors, a hypothetical cell was created with them in the system.

In the two-receptor system, equal numbers of B1 and B2 receptors were used. The B1 receptors were all precoupled, and decay of the activated receptor was through dissociation of Gq-GTP. There was no desensitization through receptor phosphorylation. The Ca^{2+} release and MLC phosphorylation profiles exhibit an elevated baseline after the peak at high ligand concentrations (Fig. 10). Although the bradykinin concentration required for this effect is nonphysiological (30 μM), the B1 receptor is selectively activated by desArg-9-bradykinin at nanomolar concentrations (Marsh and Hill, 1994), and may also exhibit constitutive activation (Leeb-Lundberg et al., 2001). Therefore, the simulation data predict that expression of the B1 receptor will change the baseline levels of MLC phosphorylation and Ca^{2+} within smooth muscle cells in the presence of selected agonists or constitutive activation.

DISCUSSION

Through computer simulation it is possible to model a complete Ca^{2+} signaling process beginning with a plasma membrane receptor and ending with a protein phosphorylation event such as myosin light chain phosphorylation. The model, as implemented in the Virtual Cell, provides multiple modules that consider multiple protein phosphorylation/

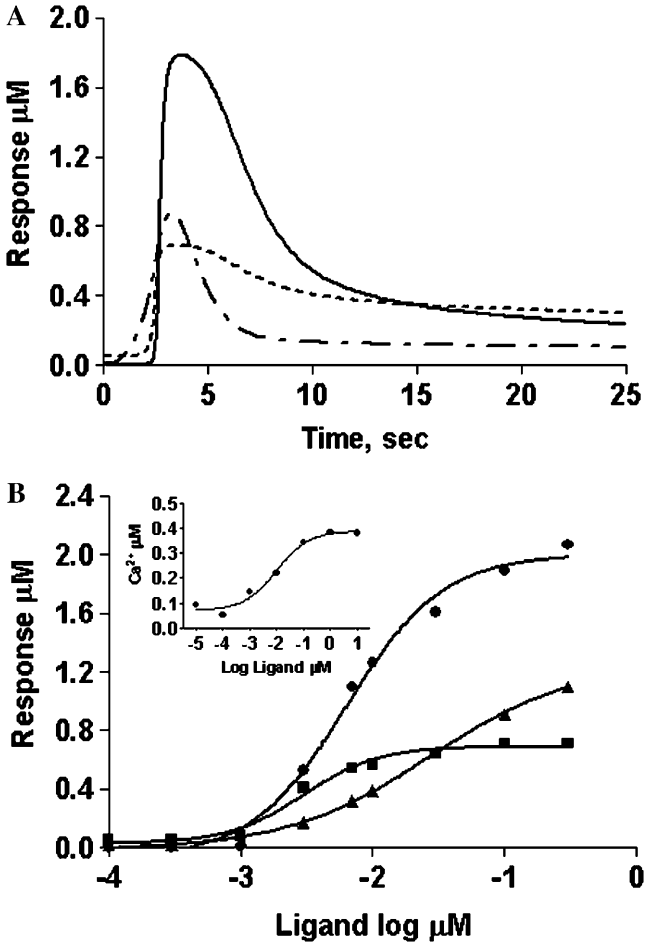

FIGURE 6 Simulation results of a time course of ligand-GPCR-activated processes. (*A*) Shown are curves for the stimulation of cells with 100 nM agonist (10× *K*d) yielding Ca^{2+}-CaM-MLCK complex formation (*solid line*), Ca^{2+} release (*dotted line*), and IP3 (*dot-dash line*). (*B*) Prediction of the ligand dependence of the peak of IP3 (*squares*), Ca^{2+} (*triangles*), and Ca^{2+}-CaM-MLCK complex (*circles*) through activation of the receptor-linked downstream processes. Inset has an experimental example of the dependence of Ca^{2+} peak on bradykinin concentration in stimulation of smooth muscle cells (adapted from Marsh and Hill, 1993).

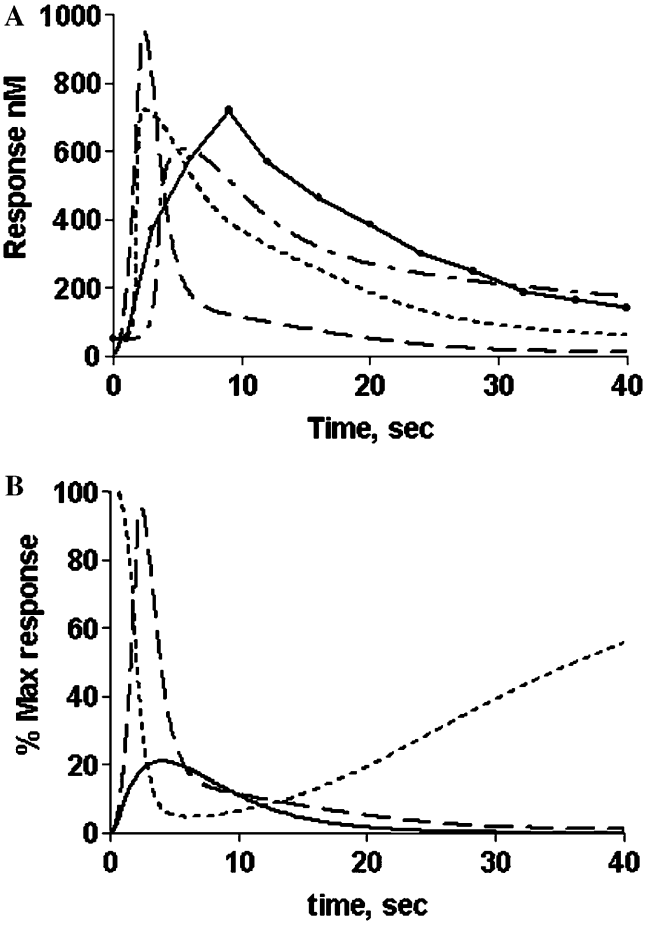

FIGURE 7 Comparison of the predicted Ca^{2+} response with experimental results. (*A*) Output from simulations of the model GPCR-coupled receptor with 100 nM agonist (10× *K*d) . IP3 (*dashed line*)-induced Ca^{2+} release (*dotted line*) in the model containing precoupled receptors is faster than that from the model without receptor precoupling (*dot-dash line*). The experimental data (*solid line with points*) is the Ca^{2+} response from smooth muscle cells stimulated with Arg-vasopressin (adapted from Simpson and Ashley, 1989). (*B*) Profile of IP3 generation (*dashed line*), PIP2 (*dotted line*), and activated PLC (*solid line*) from the precoupled receptor model initiated with 100 nM agonist. The peak of IP3 response corresponds to the peak of PLC activity and the consumption of PIP2.

dephosphorylation events initiated by the engagement of a G-protein-coupled receptor and ligand. Thus, simulations based upon the model provide a means to predict the course of these events that at defined time points can be monitored (post-reaction) using phosphorylation site-selective reagents (antibodies, phosphomotif binding proteins, etc.). Multiplex assays for analyzing the activation of selected kinases are now available (Hu et al., 2003), and real-time measurements of a few protein kinase activities are being developed (Wu et al., 2001). Thus, the Ca^{2+} signaling model presented here provides a tool for evaluating these types of data, and how changes in signaling systems will affect the measured endpoints. Now, instead of just forecasting the initial messenger production (Ca^{2+}, cyclicAMP, IP3, etc.), the signaling prototype presented here provides for coupling these messengers to multiple downstream processes simultaneously. Thus, the time course is extended to all relevant signaling events, such as kinase cascades, other second messengers, and endpoints that were not yet connected to Ca^{2+} signals. Although much work remains to be done to extend the created models to other cell types and systems, the prototype developed here serves as an extensible tool for this task.

For example, the initiating process, ligand binding to a GPCR, was formulated as a multistate collision model previously established by Linderman (Shea and Linderman, 1997). Ligand binding and receptor number data are available for several Gq-coupled receptors in native cultured cells or transfected cell lines (Nakamura et al., 1995), allowing the prediction of Ca^{2+} fluxes, IP3, and DAG generation (second messengers), and downstream endpoints.

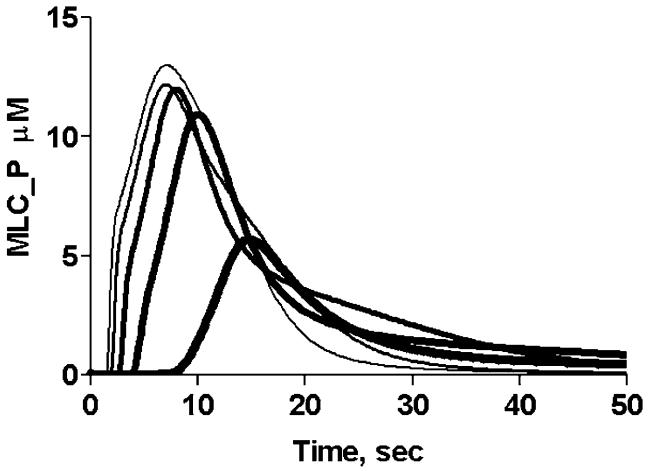

FIGURE 8 Effects of GPCR ligand/agonist concentration on the profile of MLC phosphorylation predictions. Using the generic model with receptor precoupling, the agonist concentration was varied (3–300 nM). The MLC phosphorylation profile is shown with the thickest line corresponding to 3 nM, and lines of decreasing thickness represent 10, 30, 100, and 300 nM respectively. The greatest shift in peak time occurs between the application of 3 and 30 nM agonist.

The novel aspect of the current work is the coupling of the second messengers (Ca^{2+}/DAG) to their upstream (IP3/Gq) and downstream effectors. For cytoplasmic Ca^{2+}, the primary effector is calmodulin and its target molecules, whereas with DAG, the primary signaling is through PKC. Modeling these processes required knowledge of binding parameters, kinetics, and estimates of the cellular concentrations of the key species. In cases where in vitro experimental data are available (Table 1), they are adequate for parameterization. Most of the uncertainty in the levels of lipids, phosphatases, and other species in the model are cell type-specific and may be scaled as needed without dramatically changing the qualtity of endpoint predictions.

For the simulation of the Ca^{2+} signaling process to be able to mimic cellular events, the signal control elements must be included. These include: phosphatase activities that counter activated kinases, degradation or resequestration of second messengers, and consideration of other cellular cross-talk that may influence the measured cellular endpoints. In the case of MLCK, phosphorylation at sites in the CaM-regulatory domain by CaMKII and PAK-1 decrease the Ca^{2+}-CaM sensitivity of the kinase; thus, assessment of MLCK phosphorylation state in vivo at these sites is the next step needed to refine the current model. In the companion article (Lukas, 2004), the role of phosphorylation of MLCK and several of the controlling elements for myosin phosphatase activity are expanded in the context of the model. For example, in the regulation of phosphatase activity both phosphorylation of the regulatory subunit and activation of the inhibitor protein CPI-17 are included.

The model and simulation environment developed in this work are applicable to a variety of Ca^{2+}-mobilizing GPCRs.

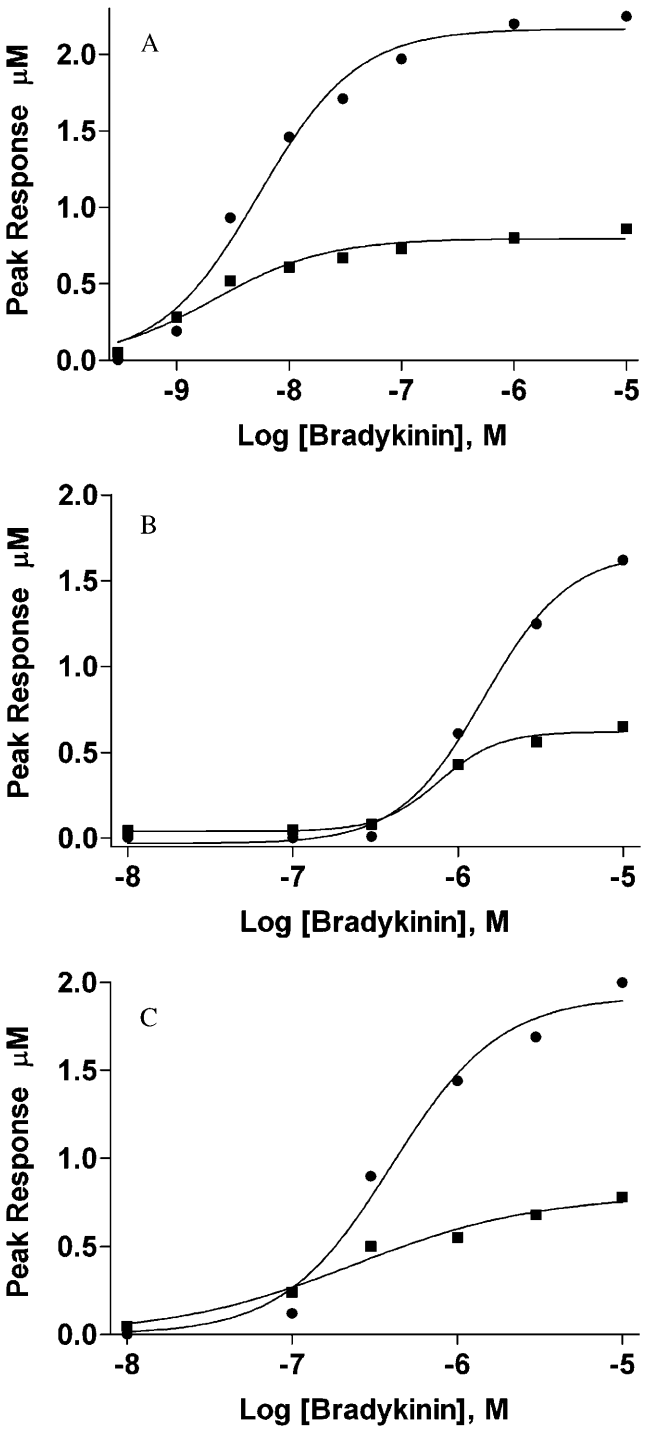

FIGURE 9 Predicted Ca^{2+}-CaM-MLCK complex formation (*circles*) and peak Ca^{2+} concentration (*boxes*) for different bradykinin receptors. (*A*) Simulated dose-response curves for the high-affinity B2 receptor using the published parameters (Table 1). (*B*) Simulated dose-response curves for the low-affinity B1 receptor with no change in receptor kinetics. (*C*) Simulated dose-response curves for the B1 receptor with a fivefold increase in the on-rate parameter.

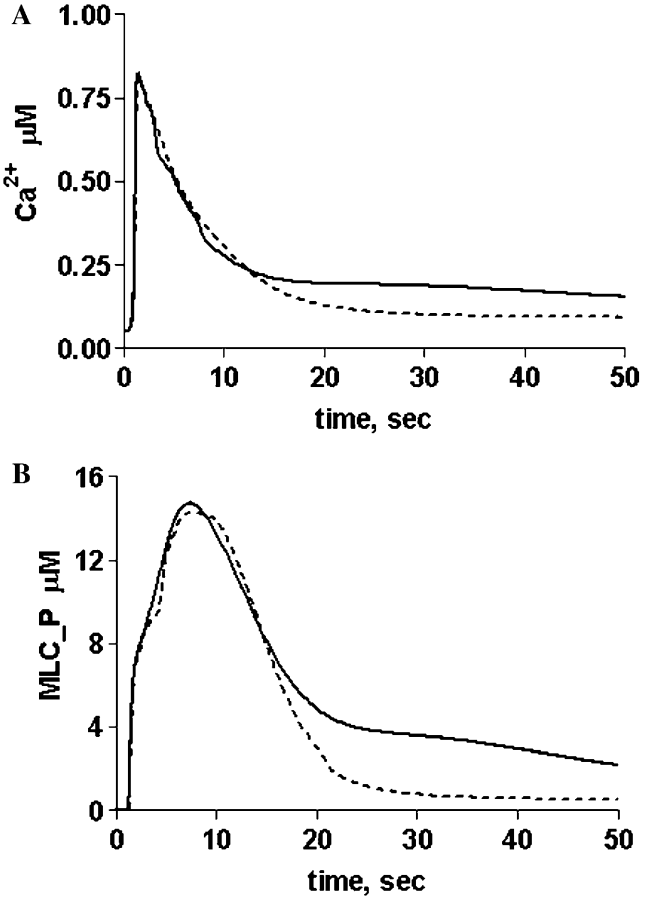

FIGURE 10 Predicted Ca^{2+} and myosin light chain phosphorylation profiles for a cell containing equal numbers of bradykinin B1 and B2 receptors. (*A*) Predicted Ca^{2+} response by application of 3 μM (*dotted line*) and 30 μM (*solid line*) of bradykinin. (*B*) Predicted MLC phosphorylation profile as a function of time with the same treatments. Note the elevated baseline (particularly at 30 μM) after the peak of Ca^{2+} or MLC phosphorylation.

Specific demonstration of predicted responses with the B1 and B2 bradykinin receptors indicates that receptor-specific parameters such as ligand-binding kinetics, mode of desensitization, and receptor number are needed to model additional receptor species. These data may be obtained experimentally using heterologous expression in cultured cells (Leeb-Lundberg et al., 2001), or through pharmacologic manipulation of native receptors (Marsh and Hill, 1993, 1994; Schaeffer et al., 2001).

CONCLUSIONS

Using the Virtual Cell environment, the current modeling effort provides a facile tool for biochemists and other life scientists to describe Ca^{2+} signal transduction processes in quantitative terms. The logical extension of the model presented here is the addition of other GPCRs that couple to other effectors such as adenylate cyclase, ion channels, etc. This will allow more robust experimental design as the simulations can be used to predict quantitative biological endpoints. Incorporation of new modules that dynamically regulate cGMP levels, RhoA and activation of other G-proteins will produce a simulation environment that couples multiple signaling pathways to convergent processes. Such efforts are currently in progress.

APPENDIX

The rate of formation of activated ligand-receptor-G-protein complex, LRG, is given by Eq. A1:

$$d[LRG]/dt = \alpha \times kf \times [L][RG] - k\mathrm{f} \times K\mathrm{d} \times [LRG] + kf \times K\mathrm{d} \times [LR][G], \quad \text{(A1)}$$

where Kd is the ligand binding constant, kf is the forward rate constant, and α is the coupling factor. In the generic model, Kd $=0.01$ μM, $\alpha = 1000$, and $k\mathrm{f} = 10 \times 10^6$ M^{-1} s^{-1}. This is an average on-rate based upon values derived for chemokine receptors (Shea and Linderman, 1997). The rate of binding of uncoupled receptors to ligand is obtained from Eq. A2:

$$d[LR]/dt = k\mathrm{f} \times [L] \times [R] - k\mathrm{f} \times K\mathrm{d} \times [LR]. \quad \text{(A2)}$$

Similarly, the rate of formation of precoupled receptors, RG, is obtained from Eq. A3:

$$d[RG]/dt = k\mathrm{f_G} \times [R][G] - K\mathrm{act} \times k\mathrm{f_G} \times [RG], \quad \text{(A3)}$$

where Kact is the equilibrium constant for receptor precoupling and $k\mathrm{f_G}$ is the forward rate constant. In the generic model, $k\mathrm{f_G}$ was set to diffusion-limited (10^8 M^{-1} s^{-1}) and Kact adjusted to obtain the desired level (25%) of precoupled receptors.

Modeling of phospholipid synthesis was accomplished using Eqs. A4–A6 to describe stimulated and basal PIP2 synthesis:

$$\mathrm{PIP2\_synthesis} = (V\mathrm{stim} + V\mathrm{basal}) \times [\mathrm{PIP}] \quad \text{(A4)}$$

$$V\mathrm{stim} = K\mathrm{stim} \times (e^{-(t-\mathrm{tau})/\mathrm{stimdecay}})\mathrm{tau} = 0.2\,\mathrm{s} \quad \text{(A5)}$$

$$V\mathrm{basal} = K\mathrm{basal} \times (-1 + e^{(\mathrm{PIP2basal}-\mathrm{PIP2})/\mathrm{PIP2basal})}). \quad \text{(A6)}$$

Phospholipase C activation was formulated using the constants in Table 2 and Eqs. A7–A8:

$$d[\mathrm{PLCact}]/dt = kfp \times [\mathrm{PLC}] \times [\mathrm{Gq\text{-}GTP}] + kfp' \times [\mathrm{Gq\text{-}GTP}][\mathrm{Ca^{2+}\text{-}PLC}] - k\mathrm{r} \times [\mathrm{PLCact}] \quad \text{(A7)}$$

$$d[\mathrm{Ca^{2+}\text{-}PLC}]/dt = k\mathrm{f}ca \times [\mathrm{PLC}] \times [\mathrm{Ca^{2+}}] - k\mathrm{f}ca \times K\mathrm{c\text{-}plc\text{-}b} \times [\mathrm{Ca^{2+}\text{-}PLC}]. \quad \text{(A8)}$$

Synthesis of IP3 and DAG was formulated using Eq. 10 and constants in Table 2:

$$d[\mathrm{IP3}]/dt = K\mathrm{cat} \times [\mathrm{PIP2}] \times [\mathrm{PLC\_act}] \times ([\mathrm{Ca^{2+}}]/(K\mathrm{c\text{-}plc\text{-}s} + [\mathrm{Ca^{2+}}]) \quad \text{(A9)}$$

The Virtual Cell Portal is provided by the National Resource for Cell Analysis and Modeling supported by National Institutes of Health grant 5P41RR013186.

REFERENCES

Adams, J. A., G. M. Omann, and J. J. Linderman. 1998. A mathematical model for ligand/receptor/G-protein dynamics and actin polymerization in human neutrophils. *J. Theor. Biol.* 193:543–560.

Black, D. J., S. B. Tikunova, J. D. Johnson, and J. P. Davis. 2000. Acid pairs increase the N-terminal Ca2+ affinity of CaM by increasing the rate of Ca2+ association. *Biochemistry.* 39:13831–13837.

Bray, D. 1997. Reductionism for biochemists: how to survive the protein jungle. *Trends. Biochem. Sci.* 22:325–326.

Davis, J. P., S. B. Tikunova, M. P. Walsh, and J. D. Johnson. 1999. Characterizing the response of calcium signal transducers to generated calcium transients. *Biochemistry.* 38:4235–4244.

Feng, J., M. Ito, K. Ichikawa, N. Isaka, M. Nishikawa, D. J. Hartshorne, and T. Nakano. 1999. Inhibitory phosphorylation site for Rho-associated kinase on smooth muscle myosin phosphatase. *J. Biol. Chem.* 274: 37385–37390.

Fink, C. C., B. Slepchenko, and L. M. Loew. 1999. Determination of time-dependent inositol-1,4,5-trisphosphate concentrations during calcium release in a smooth muscle cell. *Biophys. J.* 77:617–628.

Fink, C. C., B. M. Slepchenko, I. I. Moraru, J. Watras, J. C. Schaff, and L. M. Loew. 2000. An image-based model of calcium waves in differentiated neuroblastoma cells. *Biophys. J.* 79:163–183.

Garrad, R. C., M. A. Otero, L. Erb, P. M. Theiss, L. L. Clarke, F. A. Gonzalez, J. T. Turner, and G. A. Weisman. 1998. Structural basis of agonist-induced desensitization and sequestration of the P2Y2 nucleotide receptor. Consequences of truncation of the C terminus. *J. Biol. Chem.* 273:29437–29444.

Goldbeter, A., G. Dupont, and M. J. Berridge. 1990. Minimal model for signal-induced Ca2+ oscillations and for their frequency encoding through protein phosphorylation. *Proc. Natl. Acad. Sci. USA.* 87:1461–1465.

Haiech, J., M. C. Kilhoffer, T. J. Lukas, T. A. Craig, D. M. Roberts, and D. M. Watterson. 1991. Restoration of the calcium binding activity of mutant calmodulins toward normal by the presence of a calmodulin binding structure. *J. Biol. Chem.* 266:3427–3431.

Hu, J. H., H. Zhang, R. Wagey, C. Krieger, and S. L. Pelech. 2003. Protein kinase and protein phosphatase expression in amyotrophic lateral sclerosis spinal cord. *J. Neurochem.* 85:432–442.

Ichikawa, K., M. Ito, and D. J. Hartshorne. 1996. Phosphorylation of the large subunit of myosin phosphatase and inhibition of phosphatase activity. *J. Biol. Chem.* 271:4733–4740.

Ikebe, M., and S. Reardon. 1990. Phosphorylation of smooth muscle myosin light chain kinase by smooth muscle Ca2+/calmodulin-dependent multifunctional protein kinase. *J. Biol. Chem.* 265:8975–8978.

Illenberger, D., C. Walliser, B. Nurnberg, L. M. Diaz, and P. Gierschik. 2003. Specificity and structural requirements of phospholipase C-beta stimulation by Rho GTPases versus G protein beta gamma dimers. *J. Biol. Chem.* 278:3006–3014.

Johnson, J. D., C. Snyder, M. P. Walsh, and M. Flynn. 1996. Effects of myosin light chain kinase and peptides on Ca2+ exchange with the N- and C-terminal Ca2+ binding sites of calmodulin. *J. Biol. Chem.* 271:761–767.

Kasturi, R., C. Vasulka, and J. D. Johnson. 1993. Ca2+, caldesmon, and myosin light chain kinase exchange with calmodulin. *J. Biol. Chem.* 268:7958–7964.

Keizer, J., and G. De Young. 1994. Simplification of a realistic model of IP3-induced Ca2+ oscillations. *J. Theor. Biol.* 166:431–442.

Kenakin, T. 1997. Molecular models of drug-receptor interactions. *In* Molecular Pharmacology: A Short Course. T. Kenakin, editor. Blackwell Science, Cambridge, MA. 44–61.

Kenakin, T. 2002. Drug efficacy at G protein-coupled receptors. *Annu. Rev. Pharmacol. Toxicol.* 42:349–379.

Kenakin, T., and O. Onaran. 2002. The ligand paradox between affinity and efficacy: can you be there and not make a difference? *Trends Pharmacol. Sci.* 23:275–280.

Leeb-Lundberg, L. M., D. S. Kang, M. E. Lamb, and D. B. Fathy. 2001. The human B1 bradykinin receptor exhibits high ligand-independent, constitutive activity. Roles of residues in the fourth intracellular and third transmembrane domains. *J. Biol. Chem.* 276:8785–8792.

Lemon, G., W. G. Gibson, and M. R. Bennett. 2003a. Metabotropic receptor activation, desensitization and sequestration-I: modelling calcium and inositol 1,4,5-trisphosphate dynamics following receptor activation. *J. Theor. Biol.* 223:93–111.

Lemon, G., W. G. Gibson, and M. R. Bennett. 2003b. Metabotropic receptor activation, desensitization and sequestration-II: modelling the dynamics of the pleckstrin homology domain. *J. Theor. Biol.* 223:113–129.

Li, Y. X., and J. Rinzel. 1994. Equations for InsP3 receptor-mediated [Ca2+]i oscillations derived from a detailed kinetic model: a Hodgkin-Huxley like formalism. *J. Theor. Biol.* 166:461–473.

Lukas, T. J. 2004. A signal transduction pathway model prototype II: Application to calmodulin signaling and myosin light chain phosphorylation. *Biophys. J.* 87:1417–1425.

Marsh, K. A., and S. J. Hill. 1993. Characteristics of the bradykinin-induced changes in intracellular calcium ion concentration of single bovine tracheal smooth muscle cells. *Br. J. Pharmacol.* 110:29–35.

Marsh, K. A., and S. J. Hill. 1994. Des-Arg9-bradykinin-induced increases in intracellular calcium ion concentration in single bovine tracheal smooth muscle cells. *Br. J. Pharmacol.* 112:934–938.

Mendes, P. 1997. Biochemistry by numbers: simulation of biochemical pathways with Gepasi 3. *Trends Biochem. Sci.* 22:361–363.

Milos, M., J. J. Schaer, M. Comte, and J. A. Cox. 1988. Microcalorimetric investigation of the interaction of calmodulin with seminalplasmin and myosin light chain kinase. *J. Biol. Chem.* 263:9218–9222.

Mirzoeva, S., S. Weigand, T. J. Lukas, L. Shuvalova, W. F. Anderson, and D. M. Watterson. 1999. Analysis of the functional coupling between calmodulin's calcium binding and peptide recognition properties. *Biochemistry.* 38:3936–3947.

Mishra, J., and U. S. Bhalla. 2002. Simulations of inositol phosphate metabolism and its interaction with InsP(3)-mediated calcium release. *Biophys. J.* 83:1298–1316.

Monck, J. R., E. E. Reynolds, A. P. Thomas, and J. R. Williamson. 1988. Novel kinetics of single cell Ca2+ transients in stimulated hepatocytes and A10 cells measured using fura-2 and fluorescent videomicroscopy. *J Biol Chem.* 263:4569–4575.

Moneer, Z., and C. W. Taylor. 2002. Reciprocal regulation of capacitative and non-capacitative Ca2+ entry in A7r5 vascular smooth muscle cells: only the latter operates during receptor activation. *Biochem. J.* 362:13–21.

Moritz, A., P. N. De Graan, W. H. Gispen, and K. W. Wirtz. 1992. Phosphatidic acid is a specific activator of phosphatidylinositol-4-phosphate kinase. *J. Biol. Chem.* 267:7207–7210.

Mukhopadhyay, S., and E. M. Ross. 1999. Rapid GTP binding and hydrolysis by G(q) promoted by receptor and GTPase-activating proteins. *Proc. Natl. Acad. Sci. USA.* 96:9539–9544.

Muldoon, L. L., K. D. Rodland, M. L. Forsythe, and B. E. Magun. 1989. Stimulation of phosphatidylinositol hydrolysis, diacylglycerol release, and gene expression in response to endothelin, a potent new agonist for fibroblasts and smooth muscle cells. *J. Biol. Chem.* 264:8529–8536.

Nakamura, F., M. Kato, K. Kameyama, T. Nukada, T. Haga, H. Kato, T. Takenawa, and U. Kikkawa. 1995. Characterization of Gq family G proteins GL1 alpha (G14 alpha), GL2 alpha (G11 alpha), and Gq alpha expressed in the baculovirus-insect cell system. *J. Biol. Chem.* 270: 6246–6253.

Parnot, C., S. Miserey-Lenkei, S. Bardin, P. Corvol, and E. Clauser. 2002. Lessons from constitutively active mutants of G protein-coupled receptors. *Trends Endocrinol. Metab.* 13:336–343.

Rhee, S. G., and Y. S. Bae. 1997. Regulation of phosphoinositide-specific phospholipase C isozymes. *J. Biol. Chem.* 272:15045–15048.

Riccobene, T. A., G. M. Omann, and J. J. Linderman. 1999. Modeling activation and desensitization of G-protein coupled receptors provides insight into ligand efficacy. *J. Theor. Biol.* 200:207–222.

Rumenapp, U., M. Schmidt, S. Olesch, S. Ott, C. V. Eichel-Streiber, and K. H. Jakobs. 1998. Tyrosine-phosphorylation-dependent and rho-protein-mediated control of cellular phosphatidylinositol- 4,5-bisphosphate levels. *Biochem. J.* 334:625–631.

Schaeffer, P., M. C. Laplace, P. Savi, V. Prabonnaud, V. Salel, and J. M. Herbert. 2001. Detection of bradykinin B1 receptors in rat aortic smooth muscle cells. *Biochem. Pharmacol.* 61:291–298.

Schmidt, M., C. Bienek, U. Rumenapp, C. Zhang, G. Lummen, K. H. Jakobs, I. Just, K. Aktories, M. Moos, and C. Eichel-Streiber. 1996. A role for Rho in receptor- and G protein-stimulated phospholipase C. Reduction in phosphatidylinositol 4,5-bisphosphate by Clostridium difficile toxin B. *Naunyn Schmiedebergs Arch. Pharmacol.* 354:87–94.

Schuster, S., M. Marhl, and T. Hofer. 2002. Modelling of simple and complex calcium oscillations. From single-cell responses to intercellular signalling. *Eur. J. Biochem.* 269:1333–1355.

Shea, L., and J. J. Linderman. 1997. Mechanistic model of G-protein signal transduction. Determinants of efficacy and effect of precoupled receptors. *Biochem. Pharmacol.* 53:519–530.

Simpson, A. W., and C. C. Ashley. 1989. Endothelin evoked Ca2+ transients and oscillations in A10 vascular smooth muscle cells. *Biochem. Biophys. Res. Commun.* 163:1223–1229.

Sivakumaran, S., S. Hariharaputran, J. Mishra, and U. S. Bhalla. 2003. The Database of Quantitative Cellular Signaling: management and analysis of chemical kinetic models of signaling networks. *Bioinformatics.* 19:408–415.

Slepchenko, B. M., J. C. Schaff, J. H. Carson, and L. M. Loew. 2002. Computational cell biology: spatiotemporal simulation of cellular events. *Annu. Rev. Biophys. Biomol. Struct.* 31:423–441.

Smrcka, A. V., J. R. Hepler, K. O. Brown, and P. C. Sternweis. 1991. Regulation of polyphosphoinositide-specific phospholipase C activity by purified Gq. *Science.* 251:804–807.

Takuwa, Y., Y. Kasuya, N. Takuwa, M. Kudo, M. Yanagisawa, K. Goto, T. Masaki, and K. Yamashita. 1990. Endothelin receptor is coupled to phospholipase C via a pertussis toxin-insensitive guanine nucleotide-binding regulatory protein in vascular smooth muscle cells. *J. Clin. Invest.* 85:653–658.

Tansey, M. G., K. Luby-Phelps, K. E. Kamm, and J. T. Stull. 1994. Ca(2+)-dependent phosphorylation of myosin light chain kinase decreases the Ca2+ sensitivity of light chain phosphorylation within smooth muscle cells. *J. Biol. Chem.* 269:9912–9920.

Taylor, D. A., and J. T. Stull. 1988. Calcium dependence of myosin light chain phosphorylation in smooth muscle cells. *J. Biol. Chem.* 263: 14456–14462.

Toker, A. 1998. The synthesis and cellular roles of phosphatidylinositol 4,5-bisphosphate. *Curr. Opin. Cell Biol.* 10:254–261.

Tsvetkov, P. O., I. I. Protasevich, R. Gilli, D. Lafitte, V. M. Lobachov, J. Haiech, C. Briand, and A. A. Makarov. 1999. Apocalmodulin binds to the myosin light chain kinase calmodulin target site. *J. Biol. Chem.* 274: 18161–18164.

Weernink, P. A., Y. Guo, C. Zhang, M. Schmidt, C. Eichel-Streiber, and K. H. Jakobs. 2000. Control of cellular phosphatidylinositol 4,5-bisphosphate levels by adhesion signals and rho GTPases in NIH 3T3 fibroblasts involvement of both phosphatidylinositol-4-phosphate 5-kinase and phospholipase C. *Eur. J. Biochem.* 267:5237–5246.

Willars, G. B., S. R. Nahorski, and R. A. Challiss. 1998. Differential regulation of muscarinic acetylcholine receptor-sensitive polyphosphoinositide pools and consequences for signaling in human neuroblastoma cells. *J. Biol. Chem.* 273:5037–5046.

Wilson, D. P., C. Sutherland, and M. P. Walsh. 2002. Ca2+ activation of smooth muscle contraction: evidence for the involvement of calmodulin that is bound to the triton insoluble fraction even in the absence of Ca2+. *J. Biol. Chem.* 277:2186–2192.

Woolf, P. J., and J. J. Linderman. 2003. Untangling ligand induced activation and desensitization of G-protein-coupled receptors. *Biophys. J.* 84:3–13.

Wu, G.-Y., K. Deisseroth, and R. W. Tsien. 2001. Activity-dependent CREB phosphorylation: Convergence of a fast, sensitive calmodulin kinase pathway and a slow, less sensitive mitogen-activated protein kinase pathway. *Proc. Natl. Acad. Sci. USA.* 98:2808–2813.

Xu, C., J. Watras, and L. M. Loew. 2003. Kinetic analysis of receptor-activated phosphoinositide turnover. *J. Cell Biol.* 161:779–791.

Zhong, H., S. M. Wade, P. J. Woolf, J. J. Linderman, J. R. Traynor, and R. R. Neubig. 2003. A spatial focusing model for G protein signals. Regulator of G protein signaling (RGS) protein-mediated kinetic scaffolding. *J. Biol. Chem.* 278:7278–7284.